

Standard Article

J Vet Intern Med 2017;31:770–777

Washout Ratio in the Hepatic Vein Measured by Contrast-Enhanced Ultrasonography to Distinguish Between Inflammatory and Noninflammatory Hepatic Disorders in Dogs

K. Morishita , A. Hiramoto, A. Michishita, S. Takagi, T. Osuga, S.Y. Lim, K. Nakamura, N. Sasaki, H. Ohta, and M. Takiguchi

Background: Perflubutane microbubbles, a second-generation ultrasound contrast agent, are phagocytized by Kupffer cells. This characteristic may be useful to differentiate diffuse hepatic diseases in dogs.

Hypothesis/objectives: To determine whether the washout ratio in the hepatic vein (HV) measured by contrast-enhanced ultrasonography (CEUS) can distinguish between inflammatory and noninflammatory hepatic disorders in dogs.

Animals: Forty-one client-owned dogs with hepatic disorders including 14 with hepatitis, 7 with primary hypoplasia of the portal vein (PHPV), 9 with congenital portosystemic shunt (cPSS), and 11 with other hepatopathy were enrolled. Six dogs without hepatic disease also were evaluated as healthy controls.

Methods: Dogs with hepatic disorders were prospectively included. Contrast-enhanced ultrasonography of the HV was performed for 2 minutes. Washout ratio was defined as the attenuation rate from peak intensity to the intensity at the end of the CEUS study.

Results: Washout ratio in the hepatitis group (median, 18.0%; range, 2.0–37.0%) was significantly lower than that of the PHPV (median, 52.2%; range, 11.5–86.3%), cPSS (median, 60.0%; range, 28.6–77.4%), other hepatopathy (median, 70.5%; range, 26.6–88.4%), and normal (median, 78.0%; range, 60.7–91.7%) groups. The area under the receiver operating characteristic curve for hepatitis was 0.960, with a 95% confidence interval (CI) of 0.853–0.990. Washout ratio \leq 37.1% resulted in a sensitivity of 100% (95% CI, 78.5–100%) and specificity of 85.2% (95% CI, 67.5–94.1%) for the prediction of hepatitis.

Conclusions and Clinical Importance: Washout ratio can distinguish hepatitis from the other noninflammatory disorders with high accuracy. This result might reflect impaired Kupffer cell phagocytosis in dogs with hepatitis.

Key words: Hepatitis; Perflubutane; Portal vein hypoplasia; Portosystemic shunt.

The microcirculation of tissue can be visualized by contrast-enhanced ultrasonography (CEUS) but not by conventional color Doppler imaging. With the recent development of microbubble contrast agents, peripheral injection of microbubbles has been shown to provide a stable contrast effect for intra-abdominal organs.¹

Sonazoid^a, a second-generation contrast agent that consists of perflubutane microbubbles, produces stable real-time contrast effects. In addition to the facilitation of vascular imaging, this agent is phagocytized by

Abbreviations:

| | |
|-------|--|
| ALT | alanine aminotransferase |
| AUROC | area under the receiver operating characteristic curve |
| CEUS | contrast-enhanced ultrasonography |
| cPSS | congenital portosystemic shunt |
| HVAT | hepatic vein arrival time |
| HV | hepatic vein |
| PHPV | primary hypoplasia of the portal vein |
| PI | peak intensity |
| ROC | receiver operating characteristic |
| TIC | time-intensity curve |
| TTPP | time-to-peak phase |
| TTP | time to peak |
| WR | washout ratio |

From the Department of Veterinary Clinical Sciences, Veterinary Teaching Hospital, (Morishita, Michishita, Takagi, Nakamura); Laboratory of Veterinary Internal Medicine, Department of Veterinary Clinical Sciences, Graduate School of Veterinary Medicine, Hokkaido University, Sapporo, Hokkaido Japan (Hiramoto, Osuga, Sasaki, Ohta, Takiguchi); and the Department of Veterinary Clinical Studies, Faculty of Veterinary Medicine, Universiti Putra Malaysia, Serdang, Selangor Malaysia (Lim).

This study was performed at the Graduate School of Veterinary Medicine, Hokkaido University.

Corresponding author: M. Takiguchi, DVM, PhD, Laboratory of Veterinary Internal Medicine, Department of Veterinary Clinical Sciences, Graduate School of Veterinary Medicine, Hokkaido University, N18 W9, Sapporo, Hokkaido 060-0818, Japan; e-mail: mtaki@vetmed.hokudai.ac.jp

Submitted October 14, 2016; Revised January 24, 2017; Accepted February 2, 2017.

Copyright © 2017 The Authors. Journal of Veterinary Internal Medicine published by Wiley Periodicals, Inc. on behalf of the American College of Veterinary Internal Medicine.

This is an open access article under the terms of the Creative Commons Attribution-NonCommercial License, which permits use, distribution and reproduction in any medium, provided the original work is properly cited and is not used for commercial purposes.

DOI: 10.1111/jvim.14685

Kupffer cells,^{2,3} allowing for long-lasting parenchymal contrast enhancement of the liver.⁴ Parenchymal imaging has facilitated detection of certain liver tumors as hypoechoic defects because hepatic malignancies generally do not involve Kupffer cells,⁵ and CEUS using Sonazoid has been applied in dogs for the differentiation of malignant hepatic tumors and benign nodules.^{6,7}

Contrast-enhanced ultrasonography is used mainly to characterize the vascularity of focal liver lesions in veterinary medicine,^{6,7} but application in diffuse liver disease⁸ and other organs such as the spleen,^{9,10} pancreas,¹¹ kidney,¹² heart,¹³ lymph node,¹⁴ and brain¹⁵ has been reported in recent years. So far, we have focused on CEUS of the hepatic vein (HV). Microbubbles injected peripherally arrived in the HV much earlier in cirrhotic patients,¹⁶ and this transit time negatively correlated with the severity of liver fibrosis and the

degree of portal hypertension.^{17–19} The liver receives a dual blood supply, approximately 70–80% from the portal vein and 20–30% from the hepatic artery.²⁰ Hepatic histological changes such as fibrosis and cirrhosis, or increased portal pressure, decrease the portal blood supply. Because this decrease in total hepatic blood supply is compensated by increased arterial blood flow,^{20–23} these hemodynamic changes contribute to early hepatic vein arrival time (HVAT). Considering these findings, we evaluated CEUS of the HV for assessing the hemodynamic changes associated with chronic hepatic disease in dogs. We first defined the time-dependent parameters such as HVAT, time to peak (TTP), and time-to-peak phase (TTPP). Time to peak and TTPP were defined as the time intervals from the beginning to the peak and peak phase of the contrast effect, which purely reflect intrahepatic hemodynamics. However, by the accumulation of clinical data, we found that dogs with hepatitis tended to maintain the contrast effect of the HV when compared to dogs with noninflammatory hepatic disorders. Therefore, we defined washout ratio (WR), which represents the attenuation rate from the peak enhancement to the intensity at the end of the CEUS study, and evaluated the clinical feasibility of this modality using normal dogs and dogs with experimentally induced portal hypertension.^{24,25}

In the present study, we measured the WR values of the contrast agent for the HV in dogs with various hepatic disorders, and prospectively evaluated whether WR was a useful diagnostic aid for the differentiation of inflammatory and noninflammatory hepatic diseases in clinical settings. Concurrently, other time-dependent parameters including HVAT, TTP, and TTPP also were evaluated.

Materials and Methods

Patients

Client-owned dogs presented to Hokkaido University Veterinary Teaching Hospital, with persistently high hepatic enzyme activity in blood samples between November 2012 and May 2016, were prospectively enrolled. Informed owner consent was obtained in all cases. Dogs presenting with acute clinical signs (ie, those characteristic of conditions such as acute hepatitis, common bile duct obstruction, or rupture of the gallbladder) or having apparent hepatic tumors detected by B-mode ultrasound examination were excluded.

On the basis of the clinical findings including laboratory test results, diagnostic imaging findings, and histopathological results, dogs were divided into 4 groups: hepatitis, primary hypoplasia of the portal vein (PHPV), congenital portosystemic shunt (cPSS), and other hepatopathy. The diagnostic criterion for the hepatitis group was the presence of chronic inflammatory changes in a liver sample obtained by a Tru-cut^b biopsy, laparoscopy, or laparotomy procedure. Primary hypoplasia of the portal vein was diagnosed according to the following criteria: (1) increased total serum bile acids or blood ammonia concentration and (2) histopathological findings consistent with PHPV without the presence of cPSS. Congenital portosystemic shunt was diagnosed if a single shunt vessel was identified on computed tomography with morphological characteristics consistent with an extrahepatic cPSS²⁶ and not an acquired shunt.²⁷ Dogs with glycogen accumulation or other noninflammatory changes observed on

histopathological examination of the liver were included in the other hepatopathy group. In addition, dogs with hyperadrenocorticism with characteristic clinical signs and confirmed by adrenocorticotropic hormone (ACTH) stimulation test or low-dose dexamethasone suppression test were included in the other hepatopathy group, regardless of the presence or absence of histopathological examination.

Six dogs were evaluated as healthy controls. The data from these dogs were established in our previous research.²⁴ These laboratory-owned beagle dogs were not suffering from any known hepatic disease at the time of the study based on physical examination and abdominal ultrasound examination and had normal CBC and serum biochemistry results, including fasting and postprandial total bile acid concentrations.

Contrast-Enhanced Ultrasonography

All CEUS examinations were performed by the same sonographer (KM) with 10 years' experience performing liver ultrasound examinations. Preliminary B-mode ultrasonography was used to determine the CEUS imaging site in which the size of the HV was largest. If the HV on the right, draining from the right lateral lobe or caudate lobe, was suitable for CEUS, then the dog was positioned in left lateral recumbency with manual restraint, and the HV was identified by an intercostal approach. If the HV on the left, composed of the middle HV and left HV, was suitable, then the dog was positioned in dorsal recumbency, and the transducer was placed in the subcostal area on the left upper abdomen.

An ultrasound scanner^c with a 5- to 11-MHz broadband linear probe^d suitable for pulse subtraction imaging was used for CEUS. Imaging was performed with a low mechanical index of 0.21 and a frame rate of 23 frames per second. The contrast imaging gain was set at 80 dB, and the focus was set at a depth of 4 cm. Perfusion of the HV was evaluated after an IV bolus injection of contrast agent (0.01 mL/kg), Sonzoid^a, through a 21-gauge butterfly catheter attached to a 22-gauge IV catheter placed in the cephalic vein, which then was flushed with 2 mL heparinized saline. The dose of microbubbles was determined according to that used in our previous reports.^{11,24,25} Scanning of the HV was performed for 2 minutes, and the images were recorded in 40-second cine loops on a hard disk for further offline analysis.

Quantitative Analysis

Quantitative analysis of CEUS images was performed by 3 operators (KM, AH, and AM) by an offline image analysis system^e. This system measures intensity by a grayscale level ranging from a mean pixel value of 0 (lowest intensity) to 255 (highest intensity). One image per second for the first 60 seconds, followed by 1 image at an interval of every 5 seconds for 120 seconds, from the start of microbubble contrast agent infusion was analyzed. A region of interest as large as possible without including adjacent structures was drawn over the HV, and a time-intensity curve (TIC) was generated for each injection. The TIC depicts the change in tissue intensity over time in the region of interest. Four perfusion parameters, which were defined in our previous research,¹¹ were measured from each TIC (Fig 1). Hepatic vein arrival time was the time from contrast agent injection to 20% of peak intensity (PI). Peak intensity represents the highest value taken from each TIC. Time to peak was the time taken from 20% of PI to PI. Time-to-peak phase was the time taken from 20 to 90% of PI, which reflects the initial upslope of the TIC better than does TTP. Washout ratio was defined as (PI – the intensity at the end of the CEUS study)/PI. Washout ratio reflects the attenuation rate from PI to the intensity at the end of the CEUS study.

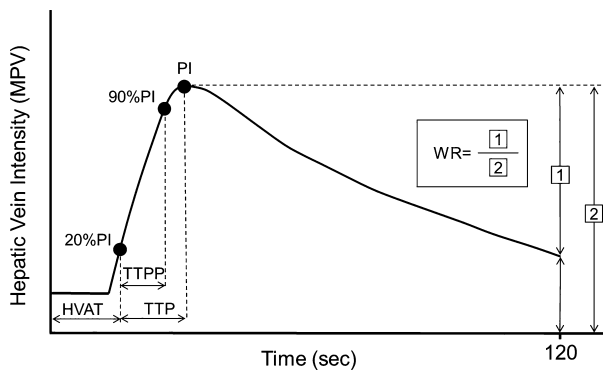


Fig 1. Schematic illustration of the time-intensity curve (TIC) and measured parameters. Hepatic vein arrival time (HVAT) was the time from contrast agent injection to 20% of peak intensity (PI, \square). Time to peak (TTP) and time-to-peak phase (TTPP) were defined as the times to reach PI and 90% PI, respectively. Washout ratio (WR) was defined as $(PI - \text{the intensity at the end of the study}) / (\text{intensity at the end of the study})$. WR reflects the attenuation rate from the PI to the intensity at the end of the study on the TIC. MPV, mean pixel value.

Statistical Analysis

Data were expressed as median values with ranges. Statistical analysis was performed with commercially available computer software^f. The overall difference among groups was determined by the Kruskal–Wallis test, and then post hoc multiple comparisons were made by the Steel–Dwass test. A receiver operating characteristic (ROC) curve was generated and the area under the receiver operating characteristic curve (AUROC) calculated to assess the performance of WR in predicting hepatitis. Sensitivity and specificity were calculated at various cutoff values. The optimal cutoff value was determined by the value with the highest Youden's index (sensitivity + specificity – 1). For all analyses, *P* values of <.05 were considered statistically significant.

Results

Study Dogs

Contrast-enhanced ultrasonography was performed in 54 dogs. No adverse effects were noted in any of the dogs. Five dogs were excluded because histopathological examination disclosed no apparent abnormalities (4 dogs with Tru-cut biopsy samples and 1 dog with laparotomy samples). Two dogs were excluded because they could not be classified adequately into any group (1 dog suspected of ductal plate malformation and the other with concomitant cholangiohepatitis and glycogen accumulation). Six dogs were excluded because quantitative analyses could not be performed because of poor image quality. Finally, a total of 41 dogs, including 14 in the hepatitis group, 7 in the PHPV group, 9 in the cPSS group, and 11 in the other hepatopathy group, were enrolled in this study.

Differences in Clinical Parameters among Groups

Diagnostic samples were obtained by Tru-cut biopsy, laparotomy, and laparoscopy procedures in 6, 4, and 4 dogs, respectively, in the hepatitis group, and in 3, 2, and 2 dogs, respectively, in the PHPV group. In the

other hepatopathy group, the 3 dogs without hyperadrenocorticism were diagnosed with samples obtained during laparoscopy.

The signalments of the dogs in each group are summarized in Table 1. The dogs in the other hepatopathy group were significantly older than those in the cPSS (Steel–Dwass; *P* = .027), PHPV (*P* = .028), and normal (*P* = .011) groups. The dogs in the hepatitis group were significantly older than those in the normal group (*P* = .028). The normal dogs were significantly heavier than those with hepatitis (Steel–Dwass; *P* = .028) or cPSS (*P* = .015). In the hepatitis group, 8 dogs were considered to have portal hypertension because of the presence of multiple tortuous vessels consistent with the morphology of acquired shunts²⁷ or ascites. Seven dogs in the hepatitis group had histological evidence of fibrosis in their liver samples, evaluated as mild fibrosis in 1 dog, moderate fibrosis in 2 dogs, and marked fibrosis in 4 dogs. In the PHPV group, 3 dogs were considered to have portal hypertension. The dogs in the other groups had no clinical findings consistent with portal hypertension.

Blood biochemistry results obtained from the medical records are summarized in Table 2. Alanine aminotransferase (ALT) activity in the hepatitis, PHPV, and other hepatopathy groups was significantly higher than that in the normal group (Steel–Dwass; *P* = .021, .028, and .010, respectively), and the ALT activity in the hepatitis group was higher than that in the cPSS group (*P* = .047). The aspartate aminotransferase activity in the hepatitis and PHPV groups was significantly higher than that in the normal group (Steel–Dwass; *P* = .014 and .043, respectively). The alkaline phosphatase activity in the hepatitis, PHPV, and the other hepatopathy groups was significantly higher than that in the normal group (Steel–Dwass; *P* = .005, .043, and .011, respectively), and the alkaline phosphatase activity in the hepatitis and the other hepatopathy groups was higher than that in the cPSS group (*P* = .008 and .025, respectively). The gamma-glutamyltranspeptidase activity in the hepatitis group was significantly higher than the activity in the PHPV, cPSS, and the normal groups (Steel–Dwass; *P* = .042, .007, and .07, respectively), and the gamma-glutamyltranspeptidase activity in the other hepatopathy group was significantly higher than that in the normal group (*P* = .025). The fasting total bile acid concentration in the cPSS group was significantly higher than the concentrations in the hepatitis and normal groups (Steel–Dwass; *P* = .037 and .020, respectively).

Differences in CEUS Parameters among Groups

The TICs for each group including the normal group are shown in Figure 2. The pixel intensity at the end of the CEUS study was highest in the hepatitis group, followed by the PHPV, cPSS, other hepatopathy, and normal groups. In particular, the hepatitis group showed little attenuation from PI. The CEUS images in a representative dog of each group are shown in Figure S1.

Results of CEUS parameters in each group are summarized in Table 3. Washout ratio in the hepatitis group was significantly lower than that in the other

Table 1. Signalments of dogs in the hepatitis, PHPV, cPSS, and other hepatopathy groups.

| | Hepatitis (n = 14) | PHPV (n = 7) | cPSS (n = 9) | Other Hepatopathy (n = 11) | Normal Dogs (n = 6) |
|----------------|---|--|---|---|------------------------------|
| Age (years)* | 10 (0–12) ^{a,b} | 2 (1–10) ^{b,c} | 5 (0–11) ^{b,c} | 11 (3–17) ^a | 2 (2–5) ^c |
| Weight (kg)* | 6.8 (3.3–11.1) ^a | 3.2 (1.7–11.4) ^{a,b} | 4.4 (2.2–8.4) ^a | 6.4 (2.2–27) ^{a,b} | 11.1 (9.7–12.5) ^b |
| Sex | Male (n = 2) Female (3) Castrated male (4) Spayed female (5) | Male (n = 5) Spayed female (2) | Male (n = 3) Female (1) Castrated male (3) Spayed female (2) | Female (n = 4) Castrated male (3) Spayed female (4) | Male (n = 3) Female (3) |
| Breed | Miniature Dachshund (n = 3), Border Collie (2), American Cocker Spaniel (1), Cavalier King Charles Spaniel (1), Chihuahua (1), English Cocker Spaniel (1), Miniature Pinscher (1), Papillon (1), Shiba (1), Toy Poodle (1), West Highland White Terrier (1) | Miniature Schnauzer (n = 2), Belgian Griffon (1), Chihuahua (1), Toy Poodle (1), Yorkshire Terrier (1), Mix (1) | Miniature Schnauzer (n = 2), Yorkshire Terrier (2), Mix (2), Chihuahua (1), Miniature Dachshund (1), Pekinese (1) | Miniature Dachshund (n = 5), Beagle (1), Chihuahua (1), Doberman (1), Papillon (1), Toy Poodle (1), Yorkshire Terrier (1) | Beagle (n = 6) |
| Classification | Chronic hepatitis (n = 6), chronic cholangiohepatitis (6), lobular dissecting hepatitis (1), copper- associated chronic hepatitis (1) | | Splenophrenic (n = 6), splenoazygous (2), right gastric-caval (1) | PDH (n = 6), AT (2), glycogen accumulation (2), copper accumulation (1) | |

PHPV, primary hypoplasia of the portal vein; cPSS, congenital portosystemic shunt; PDH, pituitary-dependent hyperadrenocorticism; AT, adrenal tumor.

Values with different superscripts are significantly different from other values, and values with the same superscripts are not different.

*Values are expressed as median (range).

groups (Steel-Dwass; vs. PHPV, $P = .027$; vs. cPSS, $P = .002$; vs. other hepatopathy, $P < .001$; vs. normal dogs, $P = .006$). The data distribution of WR in each group is shown in Figure 3. Most hepatitis patients showed a WR value of <30%. The PHPV and cPSS groups showed a similar broad distribution, whereas the distribution in the other hepatopathy group was similar to that in the normal group.

The HVAT in the hepatitis, cPSS, and other hepatopathy groups was significantly shorter than that in the normal group (Steel-Dwass; $P = .043$, $.049$, and $.024$, respectively). On the other hand, no significant difference was detected between the PHPV and the normal dogs. Time to peak and TTPP were not different among the groups.

Receiver Operating Characteristic Analysis

When the ROC curve was constructed to assess the diagnostic accuracy of WR for hepatitis, the AUROC was 0.960, with a 95% confidence interval (CI) of 0.853–0.990. Table 4 shows the results of ROC analysis with various cutoff values, which were determined by ROC curves. A WR of $\leq 37.1\%$ showed the highest Youden’s index, and resulted in a sensitivity of 100% (95% CI, 78.5–100) and specificity of 85.2% (95% CI, 67.5–94.1) for the prediction of hepatitis.

Discussion

We evaluated the differences in CEUS parameters among dogs with various hepatic disorders. As a result, we found that the WR was significantly lower in the hepatitis group than in the other groups, and may be a

useful marker to distinguish between inflammatory and noninflammatory hepatic diseases. To the best of our knowledge, WR of the HV has not been assessed previously in either human or veterinary medicine.

The disposition of perflubutane in rats after IV injection of Sonazoid has been reported.²⁸ They found that the total amount of perflubutane recovered in the analyzed tissues 5 minutes after injection was 69.2% of the injected dose and 50.7% of the injected dose was recovered in the liver.²⁸ This result indicates that metabolism by the liver largely contributes to the decrease in blood concentrations of perflubutane during the early phase. Because Sonazoid is phagocytized effectively by Kupffer cells when it passes through the sinusoids,² we considered that decreased Kupffer cell phagocytosis in the hepatitis group was the most likely reason for the lower WR results in this group.

Decreased uptake of microbubbles by Kupffer cells may be due to (1) decreased number of Kupffer cells, (2) disrupted hepatic microcirculation, and (3) impaired phagocytic function of the Kupffer cells. The number of Kupffer cells may be decreased in patients with microhepatica or in patients with chronic hepatitis if the inflammation is severe enough to induce hepatocellular necrosis or fibrosis.⁸ The hepatic microcirculation of the contrast agent may be interrupted because of narrowed sinusoids or portal branches. Moreover, intrahepatic shunts may be established in response to increased portal resistance. Intrahepatic shunts originated at zone I and diverted up to 70% of the portal venous blood from zone III regions in the rat liver after intraportal microsphere injections.²⁹ Therefore, intrahepatic shunts may cause some of the microbubbles to bypass the hepatocytes and Kupffer cells, and bypassed Sonazoid could be removed

Table 2. Blood biochemical parameters of dogs in the hepatitis, PHPV, cPSS, and other hepatopathy groups.

| | Hepatitis | | PHPV | | cPSS | | Other Hepatopathy | | Normal Dogs | |
|--------------------------------------|-------------------------------|----|-------------------------------|---|---------------------------------|---|-------------------------------|----|----------------------------|---|
| | Median (Range) | n | Median (Range) | n | Median (Range) | n | Median (Range) | n | Median (Range) | n |
| TP (RI: 5.0–7.2 g/dL) | 6.2 (4.7–7.7) | 14 | 5.5 (4.3–6.8) | 7 | 6 (4.7–7.8) | 9 | 6.8 (5.6–7.9) | 6 | 5.7 (5.1–6.2) | 6 |
| ALB (RI: 2.6–4.0 g/dL) | 2.9 (1.9–3.6) | 14 | 3.2 (1.7–3.7) | 7 | 2.7 (2.1–3.6) | 9 | 3.9 (2.8–4.4) | 6 | 3.0 (2.7–3.3) | 6 |
| ALT (RI: 17–78 IU/L) | 463 (29–>1000) ^a | 14 | 412 (95–>1000) ^{a,b} | 7 | 77 (13–282) ^{b,c} | 9 | 261 (92–>1000) ^{a,b} | 11 | 46 (28–65) ^c | 6 |
| AST (RI: 17–44 IU/L) | 100 (33–344) ^a | 13 | 87 (36–267) ^{a,b} | 7 | 39 (27–96) ^{a,b} | 8 | 46 (21–122) ^a | 11 | 32 (23–37) ^b | 6 |
| ALP (RI: 47–254 IU/L) | 1439 (335–>3500) ^a | 14 | 496 (173–1525) ^{a,b} | 7 | 235 (51–483) ^{b,c} | 9 | 2530 (233–>3500) ^a | 11 | 159 (50–233) ^c | 6 |
| GGT (RI: 5–14 IU/L) | 50 (9–238) ^a | 12 | 9 (6–49) ^{b,c} | 7 | 7 (3–10) ^{b,c} | 7 | 19 (9–523) ^{a,b} | 7 | 4 (4–7) ^c | 6 |
| T-Bil (RI: 0.1–0.5 mg/dL) | 0.7 (0.2–17.9) | 14 | 0.1 (0.1–2.2) | 7 | 0.2 (0.1–0.3) | 9 | 0.2 (0.1–0.5) | 9 | 0.3 (0.2–0.3) | 6 |
| T-CHO (RI: 111–312 mg/dL) | 285 (93–450) | 14 | 141 (35–494) | 5 | 163 (40–334) | 7 | 266 (200–432) | 5 | 167 (147–172) | 6 |
| NH ₃ (RI: 19–120 μmol/dL) | 38 (10–301) | 13 | 89 (35–124) | 3 | 102 (10–379) | 9 | 13 (0–15) | 3 | 19 (12–34) | 6 |
| TBA (RI: 0–15 μmol/dL) | 54.1 (5.4–139) ^a | 7 | 50.4 (5.9–299) ^{a,b} | 5 | 207.5 (63.6–374.2) ^b | 9 | 2.5 (2–2.9) ^{a,b} | 2 | 1.4 (0.1–7.7) ^a | 6 |

PHPV, primary hypoplasia of the portal vein; cPSS, congenital portosystemic shunt; TP, total protein; ALB, albumin; ALT, alanine aminotransferase; AST, aspartate aminotransferase; ALP, alkaline phosphatase; GGT, gamma-glutamyltranspeptidase; T-Bil, total bilirubin; T-CHO, total cholesterol; NH₃, ammonia; TBA, total bile acid; RI, reference interval.

Values with different superscripts are significantly different from other values; values with no or the same superscripts are not different.

Values are expressed as median (range).

by exhalation or uptake in other tissues, such as the spleen, kidney, and lung.²⁸ However, the distribution proportion of Sonazoid in the liver is more than half, and bypassed Sonazoid recirculated into the liver may result in a prolonged contrast effect in the HV. Impaired phagocytic function of Kupffer cells may occur in various hepatic disorders. The accumulation of the hepatic parenchyma-specific contrast agent, Levovist^g, was decreased remarkably in nonalcoholic steatohepatitis patients compared with nonalcoholic fatty liver disease patients and healthy volunteers.³⁰ Recent reports indicated that this low accumulation of contrast agent is caused mainly by decreased phagocytic capacity, and not number of Kupffer cells in animal disease models.^{31,32} Kupffer cell dysfunction has been studied mainly in relation to nonalcoholic steatohepatitis in humans, but similar imaging findings have been reported in patients with cirrhosis resulting from chronic viral hepatitis.^{33,34} Although canine Kupffer cell dysfunction in relation to hepatic disorders has never been reported, impaired phagocytic function of Kupffer cells may have contributed to lower WR in the hepatitis group in our study.

The aforementioned factors are not specific to hepatitis cases. For example, disturbed hepatic microcirculation followed by the establishment of intrahepatic shunts generally is present in PHPV, and an extrahepatic shunt in cPSS can cause some of the microbubbles to bypass the liver, similar to intrahepatic shunts. In addition, microhepatica can be present in both PHPV and cPSS. Moreover, extrahepatic factors that can decrease intrahepatic circulation, such as hypotension, congestion of the HV, and blood hyperviscosity, might impair uptake of microbubbles by Kupffer cells. Thus, although several factors can lead to decreased WR, significantly low WR in the hepatitis group in our study suggests that hepatitis is most likely to involve these intrahepatic and extrahepatic factors, followed by PHPV, cPSS, and other hepatopathy. Because approximately half of the hepatitis dogs in our study likely had portal hypertension or hepatic fibrosis, the presence of acquired shunts or fibrosis might have substantially contributed to decreased WR in this group.

The reason WR has not been assessed previously might be related to the background of the CEUS study. Hepatic vein arrival time was the first and most investigated CEUS parameter for assessing the severity of liver fibrosis.^{17,18} Some studies have measured additional parameters to improve diagnostic accuracy, including transit time between the hepatic artery and vein and the slope gradient of the hepatic artery, portal vein, and HV.^{16,35,36} However, most studies have focused on the initial upslope of the TIC, not on the attenuation of its intensity. Moreover, the difference in contrast agents could be another reason. It was reported that 99% of Sonazoid and 47% of Levovist^g were phagocytosed by Kupffer cells in vitro, whereas only 7.3% of SonoVue^h was phagocytosed.² Our study was based on the speculation that differences in Kupffer cell phagocytosis among the various hepatic disorders would result in different WR values, and this analysis by 1 of the abovementioned contrast agents would not have provided the same results.

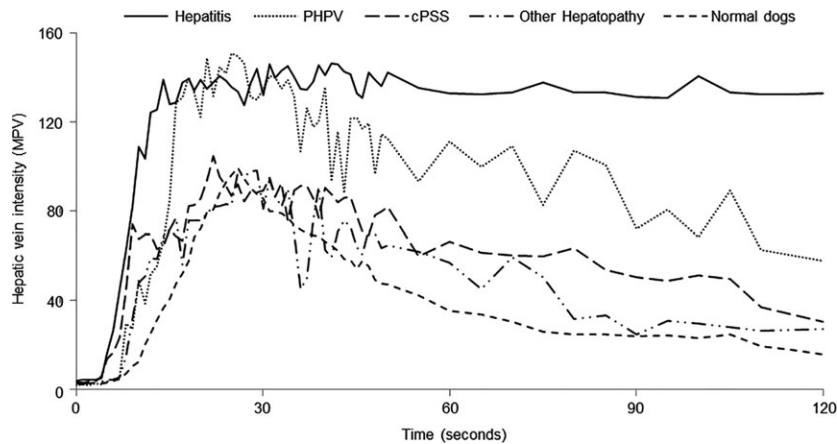


Fig 2. Time-intensity curves showing the mean pixel intensity values for each group. The pixel intensity at 120 seconds was the greatest in the hepatitis group (solid line), followed by the primary hypoplasia of the portal vein (PHPV, dotted line), congenital portosystemic shunt (cPSS, long dash line), other hepatopathy (long dash double-dotted line), and normal (dash line) groups. MPV, mean pixel value.

Table 3. Contrast-enhanced ultrasonography perfusion parameters of dogs in the hepatitis, PHPV, cPSS, other hepatopathy group, and normal groups.

| | Hepatitis (n = 14) | PHPV (n = 7) | cPSS (n = 9) | Other Hepatopathy (n = 11) | Normal Dogs (n = 6) |
|----------------|------------------------------|-------------------------------|-------------------------------|-------------------------------|-------------------------------|
| | Median (Range) | Median (Range) | Median (Range) | Median (Range) | Median (Range) |
| HVAT (seconds) | 7 (5–16) ^a | 10 (7–15) ^{a,b} | 7 (4–15) ^a | 9 (5–14) ^a | 13.5 (9–22) ^b |
| TTP (seconds) | 12 (6–19) | 9 (5–13) | 11 (3–26) | 12 (3–23) | 12.5 (6–24) |
| TTPP (seconds) | 6 (3–18) | 4 (3–11) | 5 (2–20) | 10 (3–17) | 8 (6–13) |
| WR (%) | 18.0 (2.0–37.0) ^a | 52.2 (11.5–86.3) ^b | 60.0 (28.6–77.4) ^b | 70.5 (26.6–88.4) ^b | 78.0 (60.7–91.7) ^b |

PHPV, primary hypoplasia of the portal vein; cPSS, congenital portosystemic shunt; HVAT, hepatic vein arrival time; TTP, time to peak; TTPP, time-to-peak phase; WR, washout ratio.

Values with different superscripts are significantly different from other values; values with no or the same superscripts are not different. Values are expressed as median (range).

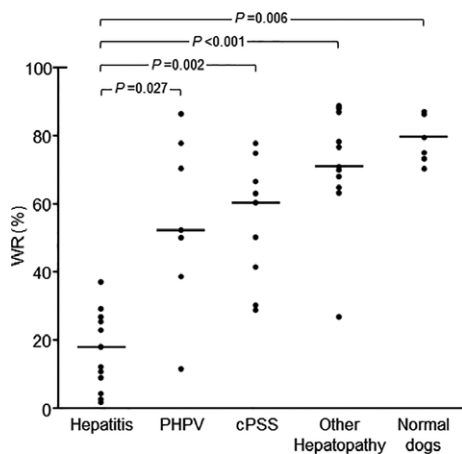


Fig 3. Plots of washout ratio (WR) in each group. Medians are indicated with horizontal lines. Horizontal bars indicate statistically significant comparisons and their P values. WR in the hepatitis group was significantly lower than that of the other groups. PHPV, primary hypoplasia of the portal vein; cPSS, congenital portosystemic shunt.

Receiver operating characteristic analysis showed that WR has good diagnostic accuracy for the diagnosis of hepatitis (Table 4). We speculate that not only the

Table 4. Diagnostic accuracy of the WR with various cutoff values for the diagnosis of hepatitis.

| Cutoff Value (%) | % Sensitivity (95% Confidence Intervals) | % Specificity (95% Confidence Intervals) | Youden's Index |
|------------------|--|--|----------------|
| ≤37.1 | 100 (78.5–100) | 85.2 (67.5–94.1) | 0.852 |
| ≤29.2 | 92.9 (68.5–98.7) | 88.9 (71.9–96.1) | 0.818 |
| ≤26.8 | 85.7 (60.1–96.0) | 92.6 (76.6–97.9) | 0.783 |
| ≤25.4 | 78.6 (52.4–94.4) | 96.3 (81.7–99.3) | 0.749 |

WR, washout ratio.

differences in WR values among the groups but also the favorable repeatability of WR itself, which was demonstrated in our previous research,²⁴ might have contributed to this finding. When the cutoff value of WR based on the ROC analysis was set at 37.1% (Table 4), 4 dogs (including 1 in the PHPV group, 2 in the cPSS group, and 1 in the other hepatopathy group) would have had false-positive diagnoses of inflammatory liver disorders. Among them, the PHPV dog showed a considerably lower WR (11.5%) than did the other PHPV dogs. This dog was clinically ill with hyperbilirubinemia and portal hypertension, and died 36 days after the CEUS examination. The owner refused postmortem

examination. Considering that the prognosis of this dog was apparently worse than that of the other PHPV dogs and that the dog exhibited clinical evidence of hepatic dysfunction and portal hypertension, its hepatic function and microcirculation might have been severely impaired, which could explain the low WR value. Alternatively, coexistence of another hepatic disease could not be excluded in this dog because one of the major limitations of hepatic biopsy procedures is sampling error in unevenly distributed lesions³⁷ and a postmortem examination could not be performed. The dog in the other hepatopathy group also showed a lower WR value (26.6%) than did the other dogs. This dog was clinically ill with remarkably high hepatic enzyme activity (ALT, >1000 IU/L). Before the first admission, the dog had been treated with prednisolone by the referring veterinarian, but the clinical signs associated with the administration of prednisolone included only polyuria and polydipsia. The histopathological diagnosis was glycogen accumulation. As the dose of prednisolone was tapered, the dog gradually recovered and its hepatic enzyme activities also decreased. We could not determine the relationship between the hepatic histopathology and clinical illness. These findings suggest that glycogen accumulation can result in decreased WR.

Time-dependent CEUS parameters including HVAT, TTP, and TTPP also were evaluated in our study. Recent research indicated shortening of the HVAT with development of liver fibrosis in a CCl₄-induced canine liver fibrosis model.³⁸ We found that the HVAT, not only in the hepatitis group, but also in the cPSS and other hepatopathy groups, was significantly shorter than in the normal dogs. This finding suggests that hemodynamic changes associated with decreased portal supply might occur in various hepatic disorders in dogs. In our previous research, we found that TTP and TTPP were shortened significantly in experimentally induced presinusoidal portal hypertension in dogs and that TTPP had significant negative correlation with the portal pressure.²⁵ Although PHPV also can induce presinusoidal portal hypertension, no statistical difference was detected between the PHPV and the normal dogs. A possible reason for this finding is that not all dogs in the PHPV group were considered to have portal hypertension. Therefore, time-dependent parameters should be used to monitor the severity of disease, not for differential diagnosis.

Our study had some limitations. First, the number of dogs used was relatively small. Second, because liver biopsy samples were not obtained from the dogs with hyperadrenocorticism, we could not rule out the coexistence of other hepatic diseases in these dogs. Third, 6 dogs were excluded because of poor image quality. This method requires clear visualization of the HV. Thus, this factor could be a major limitation in dogs with microhepatica, excessively obese dogs, and uncooperative dogs. Fourth, the operators were not blinded to each dog's clinical findings. Further blinded study by other institutions is warranted. Last, although this method has the potential to detect the inflammatory hepatic disorders, it cannot provide further information such as that yielded by histological examination of

hepatic biopsy samples. For example, the dog with hepatic copper accumulation might have required specific treatment, and this condition could only have been identified after examination of hepatic biopsy samples and copper analysis. However, CEUS is a less invasive method compared with hepatic biopsy and does not require anesthesia, and may be useful in combination with blood tests and conventional B-mode ultrasound examination in providing additional information regarding the cause of hepatic disorders in cases in which the owner does not consent to liver biopsy.

In conclusion, we showed that CEUS of the HV by parenchyma-specific contrast agents can provide useful information in differentiating nonneoplastic hepatic diseases in dogs. Washout ratio, a quantitative parameter measured from the TIC, can distinguish hepatitis from noninflammatory disorders with high accuracy. Although hepatic biopsy remains the gold standard for definitive diagnosis, this method may be a useful alternative to investigate the presence or absence of hepatitis.

Footnotes

- ^a Sonazoid, Daiichi-Sankyo, Tokyo, Japan
- ^b FINECORE, Toray medical Co Ltd, Tokyo, Japan
- ^c Aplio XG, Toshiba Medical Systems, Tochigi, Japan
- ^d PLT-704 AT, Toshiba Medical Systems
- ^e ImageJ, US National Institutes of Health, Bethesda, MD, USA
- ^f JMP Pro 12, SAS Institute Inc, Cary, NC, USA
- ^g Levovist, Schering AG, Berlin, Germany
- ^h SonoVue, Bracco, Milan, Italy

Acknowledgments

Grant support: This study was not supported by a grant or otherwise.

Conflict of Interest Declaration: Authors declare no conflict of interest.

Off-label Antimicrobial Declaration: Authors declare no off-label use of antimicrobials.

References

1. Paefgen V, Doleschel D, Kiessling F. Evolution of contrast agents for ultrasound imaging and ultrasound-mediated drug delivery. *Front Pharmacol* 2015;6:197.
2. Yanagisawa K, Moriyasu F, Miyahara T, et al. Phagocytosis of ultrasound contrast agent microbubbles by Kupffer cells. *Ultrasound Med Biol* 2007;33:318–325.
3. Watanabe R, Matsumura M, Munemasa T, et al. Mechanism of hepatic parenchyma-specific contrast of microbubble-based contrast agent for ultrasonography: Microscopic studies in rat liver. *Invest Radiol* 2007;42:643–651.
4. Watanabe R, Matsumura M, Chen CJ, et al. Gray-scale liver enhancement with Sonazoid (NC100100), a novel ultrasound contrast agent; detection of hepatic tumors in a rabbit model. *Biol Pharm Bull* 2003;26:1272–1277.
5. Hatanaka K, Kudo M, Minami Y, et al. Sonazoid-enhanced ultrasonography for diagnosis of hepatic malignancies: Comparison with contrast-enhanced CT. *Oncology* 2008;75:42–47.

6. Kanemoto H, Ohno K, Nakashima K, et al. Characterization of canine focal liver lesions with contrast-enhanced ultrasound using a novel contrast agent-sonazoid. *Vet Radiol Ultrasound* 2009;50:188–194.
7. Nakamura K, Takagi S, Sasaki N, et al. Contrast-enhanced ultrasonography for characterization of canine focal liver lesions. *Vet Radiol Ultrasound* 2010;51:79–85.
8. Liu GJ, Ji Q, Moriyasu F, et al. Value of contrast-enhanced ultrasound using perflubutane microbubbles for diagnosing liver fibrosis and cirrhosis in rats. *Ultrasound Med Biol* 2013;39:2158–2165.
9. Kanemoto H, Ohno K, Nakashima K, et al. Vascular and Kupffer imaging of canine liver and spleen using the new contrast agent Sonazoid. *J Vet Med Sci* 2008;70:1265–1268.
10. Nakamura K, Sasaki N, Murakami M, et al. Contrast-enhanced ultrasonography for characterization of focal splenic lesions in dogs. *J Vet Intern Med* 2010;24:1290–1297.
11. Lim SY, Nakamura K, Morishita K, et al. Quantitative contrast-enhanced ultrasonographic assessment of naturally occurring pancreatitis in dogs. *J Vet Intern Med* 2015;29:71–78.
12. Choi SY, Jeong WC, Lee YW, et al. Contrast enhanced ultrasonography of kidney in conscious and anesthetized beagle dogs. *J Vet Med Sci* 2016;78:239–244.
13. Ishiguro Y, Nitta N, Taniguchi N, et al. Ultrasound exposure (mechanical index 1.8) with acoustic radiation force impulse evokes extrasystolic waves in rabbit heart under concomitant administration of an ultrasound contrast agent. *J Med Ultrason* 2016;43:3–7.
14. Kogashiwa Y, Sakurai H, Akimoto Y, et al. Sentinel node biopsy for the head and neck using Contrast-enhanced ultrasonography combined with indocyanine green fluorescence in animal model: A feasibility study. *PLoS ONE* 2015;10:e0132511.
15. Seidel G, Meyer K, Algemissen C, Broillet A. Harmonic imaging of the brain parenchyma using a perflurobutane-containing ultrasound contrast agent. *Ultrasound Med Biol* 2001;27:915–918.
16. Albrecht T, Blomley MJ, Cosgrove DO, et al. Non-invasive diagnosis of hepatic cirrhosis by transit-time analysis of an ultrasound contrast agent. *Lancet* 1999;353:1579–1583.
17. Blomley MJ, Lim AK, Harvey CJ, et al. Liver microbubble transit time compared with histology and Child-Pugh score in diffuse liver disease: A cross sectional study. *Gut* 2003;52:1188–1193.
18. Lim AK, Taylor-Robinson SD, Patel N, et al. Hepatic vein transit times using a microbubble agent can predict disease severity non-invasively in patients with hepatitis C. *Gut* 2005;54:128–133.
19. Kim MY, Suk KT, Baik SK, et al. Hepatic vein arrival time as assessed by contrast-enhanced ultrasonography is useful for the assessment of portal hypertension in compensated cirrhosis. *Hepatology* 2012;56:1053–1062.
20. Kleber G, Steudel N, Behrmann C, et al. Hepatic arterial flow volume and reserve in patients with cirrhosis: Use of intra-arterial Doppler and adenosine infusion. *Gastroenterology* 1999;116:906–914.
21. Rocheleau B, Ethier C, Houle R, et al. Hepatic artery buffer response following left portal vein ligation: Its role in liver tissue homeostasis. *Am J Physiol* 1999;277:G1000–G1007.
22. Leen E, Goldberg JA, Anderson J, et al. Hepatic perfusion changes in patients with liver metastases: Comparison with those patients with cirrhosis. *Gut* 1993;34:554–557.
23. Lauth WW. Mechanism and role of intrinsic regulation of hepatic arterial blood flow: Hepatic arterial buffer response. *Am J Physiol* 1985;249:G549–G556.
24. Morishita K, Hiramoto A, Osuga T, et al. Contrast-enhanced ultrasonography of the hepatic vein in normal dogs. *J Vet Med Sci* 2017;78:1753–1758.
25. Morishita K, Hiramoto A, Osuga T, et al. Preliminary assessment of contrast-enhanced ultrasonography of the hepatic vein for detection of hemodynamic changes associated with experimentally induced portal hypertension in dogs. *Am J Vet Res In press*.
26. Kraun MB, Nelson LL, Hauptman JG, Nelson NC. Analysis of the relationship of extrahepatic portosystemic shunt morphology with clinical variables in dogs: 53 cases (2009–2012). *J Am Vet Med Assoc* 2014;245:540–549.
27. Bertolini G. Acquired portal collateral circulation in the dog and cat. *Vet Radiol Ultrasound* 2010;51:25–33.
28. Toft KG, Hustvedt SO, Hals PA, et al. Disposition of per-fluorobutane in rats after intravenous injection of Sonazoid. *Ultrasound Med Biol* 2006;32:107–114.
29. Li X, Benjamin IS, Naftalin R, et al. Location and function of intrahepatic shunts in anaesthetized rats. *Gut* 2003;52:1339–1346.
30. Iijima H, Moriyasu F, Tsuchiya K, et al. Decrease in accumulation of ultrasound contrast microbubbles in non-alcoholic steatohepatitis. *Hepato Res* 2007;37:722–730.
31. Yoshikawa S, Iijima H, Saito M, et al. Crucial role of impaired Kupffer cell phagocytosis on the decreased Sonazoid-enhanced echogenicity in a liver of a nonalcoholic steatohepatitis rat model. *Hepato Res* 2010;40:823–831.
32. Tsujimoto T, Kawaratani H, Kitazawa T, et al. Decreased phagocytic activity of Kupffer cells in a rat nonalcoholic steatohepatitis model. *World J Gastroenterol* 2008;14:6036–6043.
33. Park J, Cho J, Kwon H, et al. Liver function assessment using parenchyma-specific contrast-enhanced ultrasonography. *Ultrasound Med Biol* 2016;42:430–437.
34. Tonan T, Fujimoto K, Qayyum A, et al. Correlation of Kupffer cell function and hepatocyte function in chronic viral hepatitis evaluated with superparamagnetic iron oxide-enhanced magnetic resonance imaging and scintigraphy using technetium-99 m-labelled galactosyl human serum albumin. *Exp Ther Med* 2011;2:607–613.
35. Sugimoto H, Kaneko T, Hirota M, et al. Earlier hepatic vein transit-time measured by contrast ultrasonography reflects intrahepatic hemodynamic changes accompanying cirrhosis. *J Hepato Res* 2002;37:578–583.
36. Goto Y, Okuda K, Akasu G, et al. Noninvasive diagnosis of compensated cirrhosis using an analysis of the time intensity curve portal vein slope gradient on contrast-enhanced ultrasonography. *Surg Today* 2014;44:1496–1505.
37. Webster CRL. Clinical signs, and physical findings in hepatobiliary disease. In: Ettinger SJ, Feldman EC, eds. *Textbook of Veterinary Internal Medicine*, 7th ed. St. Louis, MO: Saunders Elsevier; 2010:1612–1625.
38. Liu H, Liu J, Zhang Y, et al. Contrast-enhanced ultrasound and computerized tomography perfusion imaging of a liver fibrosis-early cirrhosis in dogs. *J Gastroenterol Hepato Res* 2016;31:1604–1610.

Supporting Information

Additional Supporting Information may be found online in the supporting information tab for this article:

Fig. S1. Color Doppler and contrast-enhanced ultrasonography (CEUS) images of the hepatic vein (HV) in a representative dog of the hepatitis group (A–D), primary hypoplasia of the portal vein (PHPV) group (E–H), congenital portosystemic shunt (cPSS) group (I–L), and other hepatopathy group (M–P).